SHOCK, Vol. 60, No. 4, pp. 503–516, 2023

OPEN

A TRANSCRIPTOMIC APPRECIATION OF CHILDHOOD MENINGOCOCCAL AND POLYMICROBIAL SEPSIS FROM A PRO-INFLAMMATORY AND TRAJECTORIAL PERSPECTIVE, A ROLE FOR VASCULAR ENDOTHELIAL GROWTH FACTOR A AND B MODULATION?

Asrar Rashid,*† Berit S. Brusletto,‡ Feras Al-Obeidat,§ Mohammed Toufiq,‖ Govind Benakatti¶** Joe Brierley,** Zainab A. Malik,†† Zain Hussain,‡‡ Hoda Alkhazaimi,§§ Javed Sharief,† Raziya Kadwa,† Amrita Sarpal,‖‖¶¶ Damien Chaussabel,‖ Rayaz A. Malik,¶¶*** Nasir Quraishi,††† Praveen Khilnani,¶ Syed A. Zaki,‡‡‡ Rashid Nadeem,§§§ Guftar Shaikh,‖‖‖ Ahmed Al-Dubai,* Wael Hafez,¶¶¶† and Amir Hussain***

**School of Computing, Edinburgh Napier University, Edinburgh, United Kingdom; †NMC Royal Hospital, Abu Dhabi, United Arab Emirates; ‡The Blood Cell Research Group, Department of Medical Biochemistry, Oslo University Hospital, Ullevål, Norway; §College of Technological Innovation at Zayed University, Abu Dhabi, United Arab Emirates; ‖The Jackson Laboratory for Genomic Medicine Farmington, Connecticut, USA; ¶Medanta Gururam, Delhi, India; **Great Ormond Street Children's Hospital, London, United Kingdom; ††College of Medicine, Mohammed Bin Rashid University of Medicine and Health Sciences, Dubai, United Arab Emirates; ‡‡Edinburgh Medical School, University go Edinburgh, Edinburgh, United Kingdom; §§New York University, Abu Dhabi, United Arab Emirates; ‖‖Sidra Medicine, Doha, Qatar; ¶¶Weill Cornell Medicine-Qatar, Doha, Qatar; ***Institute of Cardiovascular Science, University of Manchester, Manchester, United Kingdom; †††Centre for Spinal Studies & Surgery, Queen's Medical Centre, The University of Nottingham, Nottingham, United Kingdom; ‡‡‡All India Institute of Medical Sciences, Hyderabad, India; §§§Dubai Hospital, Dubai, United Arab Emirates; ‖‖‖Endocrinology, Royal Hospital for Children, Glasgow, United Kingdom; and ¶¶¶Medical Research Division, Department of Internal Medicine, The National Research Centre, Cairo, Egypt and ****Yas Clinic, Abu Dhabi, United Arab Emirates*

Received 20 Apr 2023; first review completed 12 May 2023; accepted in final form 19 Jul 2023

ABSTRACT—This study investigated the temporal dynamics of childhood sepsis by analyzing gene expression changes associated with proinflammatory processes. Five datasets, including four meningococcal sepsis shock (MSS) datasets (two temporal and two longitudinal) and one polymicrobial sepsis dataset, were selected to track temporal changes in gene expression. Hierarchical clustering revealed three temporal phases: early, intermediate, and late, providing a framework for understanding sepsis progression. Principal component analysis supported the identification of gene expression trajectories. Differential gene analysis highlighted consistent upregulation of vascular endothelial growth factor A (VEGF-A) and nuclear factor κB1 (NFKB1), genes involved in inflammation, across the sepsis datasets. NFKB1 gene expression also showed temporal changes in the MSS datasets. In the postmortem dataset comparing MSS cases to controls, VEGF-A was upregulated and VEGF-B downregulated. Renal tissue exhibited higher VEGF-A expression compared with other tissues. Similar VEGF-A upregulation and VEGF-B downregulation patterns were observed in the cross-sectional MSS datasets and the polymicrobial sepsis dataset. Hexagonal plots confirmed VEGF-R (VEGF receptor)–VEGF-R2 signaling pathway enrichment in the MSS cross-sectional studies. The polymicrobial sepsis dataset also showed enrichment of the VEGF pathway in septic shock day 3 and sepsis day 3 samples compared with controls. These findings provide unique insights into the dynamic nature of sepsis from a transcriptomic perspective and suggest potential implications for biomarker development. Future research should focus on larger-scale temporal transcriptomic studies with appropriate control groups and validate the identified gene combination as a potential biomarker panel for sepsis.

KEYWORDS—Gene expression; proinflammation; sepsis; septic shock; temporal sepsis; VEGF-A; VEGF-B

INTRODUCTION

The global burden of pediatric sepsis is substantial, with 20 million cases yearly (1) and 2.9 million deaths in those younger than 5 years worldwide. Early detection and rapid intervention are lifesaving, thus necessitating evidence-based guidelines to optimize early interventions to improve sepsis-related outcomes. However, such efforts have yet to improve sepsis mortality significantly (2). For neonates, the estimated number of deaths annually

Address reprint requests to Asrar Rashid, MBChB, FRCPCH, MBA, Department of Computer Science, Edinburgh Napier University, Merchiston Campus, 10 Colinton Road, Edinburgh, Scotland, EH10 5DT, UK. E-mail: asrar@medicalbrainbox.com

Datasets selected for analysis in this article were from gene expression microarray data available from public repositories. Readers can access the data from the online European Bioinformatics Information database as a part of the European Molecular Biology Laboratory (https://www.ebi.ac.uk) and the National Library of Medicine GEO Dataset Repository (https://www.ncbi.nlm.nih.gov). There were no restrictions to data access from the aforementioned repositories.

The article was waived from review by the hospital Central Scientific Committee and the Research and Ethics Committee, given the secondary analysis of data from primary studies.

Financial support was not required for this study.

The authors report no conflicts of interest.

A video summary of the article is provided.

Author Contributions: AR conceived and designed the experiments; performed the experiments, analyzed the data; contributed analysis, methods, and tools; and wrote the first draft of the manuscript. BSB, FA, MT, GB, JB, ZAM, ZH, HA, JS, RK, AS, DC, RAM, NQ, PK, SAZ, RN, GS, AA, WH, and AH revised the manuscript critically for importance and intellectual content.

Supplemental digital content is available for this article. Direct URL citation appears in the printed text and is provided in the HTML and PDF versions of this article on the journal's Web site (www.shockjournal.com).

DOI: 10.1097/SHK.0000000000002192

was estimated by Fleischmann-Struzek et al. (3) as a part of a systematic analysis, calculating 3 million cases annually.

In adults, a secondary analysis of 1,332 participants in the ARISE (Australian Resuscitation in Sepsis Evaluation) study showed that infected patients with isolated hyperlactatemia had worse 90-day mortality than those with isolated hypotension (4). This suggests that metabolic derangement associated with sepsis leading to high serum lactate may be a more important determinant of mortality than hemodynamic dysfunction. The cellular effects of sepsis/septic shock are life-threatening and are mediated by several pathogen-induced proinflammatory cytokines. Meningococcal sepsis, caused by the gram-negative bacteria *Neisseria meningitidis*, is prototypical of septic shock dynamics. LPS, an important outer membrane antigen of gram-negative bacteria (5), overburdens the host immune system and elicits a wide array of inflammatory cascade resulting in septic shock (6). Using transcriptional information, a temporal-spatial trajectory has been described in infants with septic shock (7). TNF-α, a key cytokine implicated in sepsis pathogenesis, is known to activate nuclear factor κB subunit (NF-κB) (8) a key regulator of gene expression (GE) of proinflammatory cytokines in innate and adaptive immune cells (8). Nuclear factor κB activation results in the release of IL-6, activation of STAT-3, and other proinflammatory molecules such as vascular endothelial growth factor (VEGF) (9). Vascular endothelial growth factor A is a known proangiogenic and proinflammatory agent with a complex role in the inflammatory cascade. Vascular endothelial growth factor A is shown to stimulate the production and release of various cytokines such as TNF, NF-κB, IL-4, IL-6, monocyte chemotactic protein 1, and so on and vice versa (10–15). Wang and Yang (16) demonstrated TNF-α increasing VEGF-A expression resulting in increased cell migration and angiogenic differentiation in human fibroblasts. Vascular endothelial growth factor is an important determinant of sepsis morbidity and mortality (17) and a marker of inflammation and a potential therapeutic target (18). Vascular endothelial growth factor B, like VEGF-A, belongs to the VEGF family and, like VEGF-A, binds to the VEGF receptor 1 (VEGF-R1). However, VEGF-B has actions counter to that of VEGF-A, with studies suggesting its role as a vascular survival factor safeguarding endothelial cells, smooth muscle, and also cardioprotection (19–21).

Considering the diffuse endothelial dysfunction and vascular leakage; key in the pathogenesis of sepsis, septic shock, and multiorgan dysfunction; restoring vascular integrity during the recovery phase; and the close relation of VEGFs with endothelium and vascular health, we believe temporal dynamics of VEGF-A and VEGF-B in sepsis could potentially provide important insights on sepsis evolution and have the potential for biomarking and as a therapeutic target.

We aimed to study time-related sepsis dynamics from the GE perspective. Also, an objective was to appreciate differential GE changes in TNF-α (TNF), NFKB1, and VEGF-A and VEGF-B genes. The methodology was based on our findings in Kawasaki disease–associated inflammation, which has shown consistent acute upregulation of TNF, NFKB1, and VEGF-A genes and the downregulation of VEGF-B GE in acute Kawasaki disease (22). In this study, we performed transcriptomic analysis of longitudinal and cross-sectional datasets of childhood meningococcal to evaluate temporal dynamics. Finally, a temporal polymicrobial dataset was selected to evaluate GE changes in the broader context of sepsis.

METHODS

Systematic transcriptome data search and preprocessing

A systematic search of publicly available online repositories from Gene Expression Omnibus datasets—National Center for Biotechnology Information (https://www.ncbi.nlm.nih.gov/geo/) (23) and the European Molecular Biology Laboratory-Bioinformatics Institute (EMBL-BI) (https://www.ebi.ac.uk/ebisearch/about) was undertaken (Fig. 1). Thus, clinical datasets involving temporal transcriptomic sepsis studies in children were selected (Table 1). The search terms "meningococcal sepsis" and "meningococcal shock" were parsed through the Gene Expression Omnibus Gene Expression Omnibus database and EMBL-EBI ArrayExpress, leading to 64 and 5 datasets in each. This was followed by the term "meningococcal transcriptome," resulting in eight and two datasets. Finally, two temporal datasets, E-MEXP-3850 (Kwan dataset) and GSE11755 (Emonts dataset), and two nontemporal datasets, GSE141864 (Brusletto dataset) and GSE80496 (Wright dataset), were included in the final analysis, after excluding comparative genomic hybridization by array, proteomic profiling by array, duplicates, *in vitro* studies, and nonhuman organism experiments. Temporal "polymicrobial" sepsis transcriptome studies using key words "pediatric sepsis and septic shock" and GE profiling by array were searched. The initial search resulted in 80 datasets from the two databases. Finally, one dataset GSE13904 (Wong dataset), of 29 (Gene Expression Omnibus n = 9 and EBI n = 20), was included in the final analysis after the exclusion strategy outlined in Figure 1. Table 1 summarizes the clinical sepsis datasets included for final analysis.

Demographic comparisons between Kwan and Emonts datasets are shown (Table 2). The Kwan dataset (24) has blood sampled during the first 48 h of admission to the pediatric intensive care unit (PICU) with meningococcal sepsis, whereas Emonts covered 72 h (28). According to the systematic search, these were the only two temporal transcriptomic datasets in the clinical literature with multiple sampling in children with sepsis over the first 48 to 72 h. Patients in the Kwan dataset were numbered 1 to 5 (P1 to P5); in the Emonts dataset, patients were labeled 1 to 6 (P1 to P6). An arbitrary time point was designated as time 0 ($T = 0$) at the time of PICU admission and was used in both studies. The other two meningococcal sepsis shock (MSS) disease datasets are cross-sectional studies, GSE80496 (Wright dataset) and GSE141864 (Brusletto dataset), comparing meningococcal sepsis ± meningitis with controls. The Brusletto dataset is from the end-stage meningococcal disease from postmortem samples, focusing on transcriptomic changes in various organs (heart, liver and kidney) and immune cells (whole blood, lymphocytes, and monocytes). The polymicrobial sepsis dataset GSE13904 (Wong dataset) is also a temporal dataset that compared sepsis with septic shock, systemic inflammatory response syndrome (SIRS), and controls from day 1 (D1) to day 3 (D3). The datasets were first inspected for data processing methods indicated by the author(s), and appropriate normalization and log 2 transformation were applied as required using R script.

Gene Ontology analyses

Qlucore Omics Explorer (QOE) version 3.1 software (Qlucore AB, Lund, Sweden) was used to analyze the differential expression of genes. Box plots were used to illustrate differences in GE in QOE, with the *y*-axis plots showing log 2 normalized GE values. The data were centered to zero (mean) and scaled to variance 1. Gene set expression analysis (GSEA) was used to determine *a priori*–defined set of genes that showed statistically significant differences between two biological states (29). The MSigDB (Molecular Signatures Database) from the Broad Institute website (www.gsea-msigdb.org) was searched for human gene sets using keywords ("VEGF," "TNF," and "NFKB1"), and corresponding gene ranks were then downloaded. In QOE, the default settings were used for GSEA (min match set size = 15, max match set size = 500, permutations = 1,000, permutation method = sample, enrichment weight = 1). The data were preprocessed using the mean expression value of multiple probe IDs that matched an official gene symbol, and a net enrichment score was calculated. This value was considered to represent the expression intensity of the corresponding gene symbol. ANOVA and Student *t* tests were undertaken for intergroup comparisons. False discovery rate (FDR) and the familywise error rate were used for statistical analysis, with familywise error rate using the Bonferroni correction. A *q* (FDR) value of 0.25 was used for principal component analysis (PCA) and GSEA exploration to circumvent the small sample size problem. Other platforms used for gene enrichment included ShinyGo (30) and g:Profiler (31).

Transcript time course analysis

Transcript time course analysis (TTCA) R software was used for temporal data analysis (32). The Kwan dataset's last sample (at the 48-h collection point) was referred to as a constant or control. Emonts had age- and gender-matched controls. The Kyoto Encyclopedia of Genes and Genomes (KEGG) database (33) was used to obtain curated genes for VEGF-associated signaling, apoptosis, complement, and coagulation. The Hugo database (34) curated the heat shock protein genes, including HSPBAP1, zinc finger, and metallothionein genes. Simple overrepresentation analyses (*via* hypergeometric-distribution–based testing) were performed using

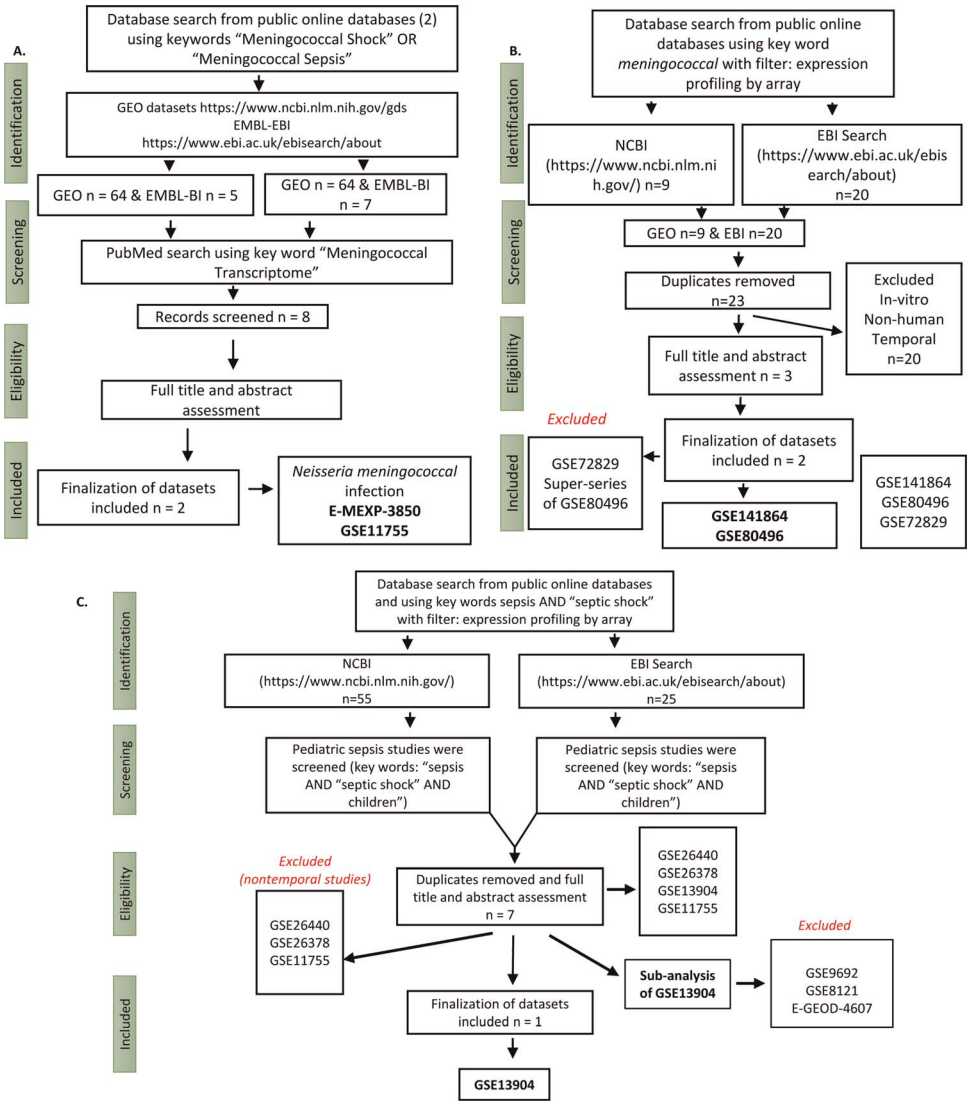

FIG. 1. **Search of publicly available databases for transcriptional studies in childhood meningococcal sepsis and polymicrobial sepsis**. This figure displays the approach to select the sepsis datasets used in this article. Two public databases were utilized, namely, the NCBI GEO database and the EMBL-EBI ArrayExpress. The selection process for publicly available temporal *Neisseria* meningococcal transcriptomic datasets is depicted in A. A search term, "meningococcal shock," was used to parse through the NCBI GEO database (yielding 64 datasets) and the EMBL-EBI ArrayExpress (yielding five datasets). The term "meningococcal sepsis" was used in both databases, resulting in seven datasets from EMBL-EBI ArrayExpress and 64 datasets from NCBI GEO. In addition, the term "meningococcal transcriptome" was searched in PubMed, assessing eight datasets. These searches yielded two publicly available datasets, E-MEXP-3850 (Kwan Dataset) and GSE11755 (Emonts dataset), for analysis. Furthermore, the selection process for nontemporal publicly available *Neisseria* meningococcal transcriptomic datasets is illustrated in B. Using "meningococcal" as the key term and "expression profiling by array" as the study type, a total of 29 datasets were identified from the NCBI GEO (n = 9) and EMBL-EBI ArrayExpress (n = 20) searches. The EMBL-EBI search initially yielded larger datasets (n = 2,433); however, irrelevant datasets and study types were excluded, resulting in 20 datasets for further screening. After removing duplicates, a total of 23 datasets remained. *In vitro* studies, experiments with nonhuman organisms, and temporal studies were excluded, leaving three datasets eligible for final selection. The objective was to select clinical transcriptomic studies on meningococcal infection with septic shock manifestation and transcriptome profiles of children with a bacterial infection. With this objective in mind, two datasets, GSE141864 (Brusletto dataset) and GSE80496 (Wright dataset), were selected. The super series GSE72829 with subseries GSE80496 was excluded as GSE80496 contained the desired meningococcal dataset. Lastly, C represents the selection process for temporal polymicrobial studies. Pediatric sepsis datasets obtained from the two online public databases using gene expression and profiling by array were initially searched for sepsis and septic shock, resulting in 80 datasets. The NCBI search included the following datasets: GSE26440, GSE26378, GSE13904, GSE11755, GSE9692, GSE8121, and GSE4607. The EBI search yielded GSE13904, GSE8121, GSE9692, GSE11755, and GSE4607. Duplicate studies were accounted for, resulting in seven eligible datasets (GSE26440, GSE26378, GSE13904, GSE11755, GSE9692, GSE8121, and GSE4607) for genomic expression analysis. Nontemporal studies were excluded from further analysis. In addition, substudies (GSE9692, GSE8121, and GSE4607) were deselected because they were included in the main study GSE13904 (the "Wong" dataset). EMBL-BI, the European Bioinformatics Institute; NCBI GEO, National Center for Biotechnology Information Gene Expression Omnibus.

the TTCA results. This resulted in significant genes related to "consensus," "early response," "middle response," "late response," "complete response," "dynamic," and "MaxDist." Similarly, pathfindR software (35) was used to analyze the genes from TTCA. KEGG pathway and Gene Ontology (36) Biological Process (GO-BP) enrichment analysis were undertaken using Enrichr (37).

Enrichr

Enrichr is an enrichment tool that allows the pasting of gene lists onto its online platform. On enrichment, there is a connection to Appyter tools allowing the illustration of the data in bar charts and hexagon plots.

TABLE 1. **Summary of clinical sepsis datasets for analysis**

Accession number*	Label	Platform	Study design	n†	Ref‡
E-MEXP-3850	Kwan	Microarray: Affymetrix Human Gene 1.0 ST Arrays	Blood was sampled at six time points during the 48 h in PICU in children	5	Kwan et al. (24), 2013
GSE11755	Emonts	Microarray: Affymetrix Human Genome U133 Plus 2.0 Array	Case-control study Children with meningococcal sepsis (n = 6) compared with controls (n = 4)	10	NA
GSE80496	Wright	Microarray: Illumina HumanHT-12 V3.0 bead chip	Case-control study Meningococcal sepsis (n = 21), meningococcal sepsis with meningitis (n = 3) and controls (n = 21)	45	Herberg et al. (25), 2016
GSE141864	Brusletto	Microarray: Affymetrix Human Transcriptome Array 2.0	Case-control study Meningococcal septic shock (n = 5) vs. control (n = 2)	7	Brusletto et al. (26), 2020
GSE13904	Wong	Microarray: Affymetrix Human Genome U133 Plus 2.0 Array	Case-control prospective observational study, normal controls (n = 18), SIRS (n = 22), sepsis (n = 32), septic shock (n = 67) (day 1)	139	Wong et al. (27), 2009

All human datasets were quantile normalized as a part of the data prepossessing. Each dataset is given a label for use throughout the article. Datasets included children admitted to the PICU. No publication reference for the Emonts dataset, which was therefore marked as NA. The selected datasets were named for readership ease according to the first author of the associated publication or designated person on the online repository.

*NCBI and EMBL-BI data repositories.

†n is the number of patients.

‡Ref is the reference literature pertaining to the study containing the dataset.

EMBL-BI, the European Bioinformatics Institute; NA, not available; NCBI GEO, National Center for Biotechnology Information Gene Expression Omnibus; PICU, pediatric intensive care unit; SIRS, systemic inflammatory response syndrome.

RESULTS

Time-series analysis

Principal component analysis of GE datasets from infants with MSS from Kwan and Emonts studies showed GE transitions from an early to a late stage. Figure 2 (A–D) illustrates the PCA plots and heat maps on gene transitions across different time points from zero to 48 h in meningococcal sepsis. Multigroup (ANOVA) temporal analysis of the Kwan dataset showed the expression levels of 728 genes defining differences between time points ($P < 0.01$). The PCA plot (Fig. 2A) shows the time as the most important component in differences between samples (principal

TABLE 2. **Demographic comparison of Kwan versus Emonts**

Patient identifier	1	2	3	4	5	1	2	3	4	5	6	*P* value comparison*
Mortality (at 28 d)	Died	Alive	Alive	Alive	Alive	Alive	Alive	Alive	Alive	Alive	Alive	
Neisseria meningococcal serotype	Negative culture (presumes meningococcal sepsis)	GpB	GpB	GpB	GpB	GpB	GpB	GpB	PCR negative	GpB	GpB	
Title	1 N	2 N	3 N	4 N	5 N	1R	2R	3R	4R	5R	6R	
DIC	Y	Y	Y	Y	Y	Y	Y	N	Y	Y	N	
Mechanical ventilation	Y	Y	Y	Y	Y	Y	Y	Y	Y	Y	Y	
Gender	Female	Female	Female	Male	Male	Male	Male	Male	Male	Male	Male	
Protein C	Y	N	N	N	N	N	N	N	N	N	N	
Hospital	Kwan	Kwan	Kwan	Kwan	Kwan	Emonts	Emonts	Emonts	Emonts	Emonts	Emonts	
No. samples taken	5	5	5	5	5	4	4	4	4	4	4	
Age (y)	1.08	0.83	1.83	2	0.75	5.06	1.37	1.79	2.09	1.51	8.04	0.13
Duration of PICU admission (d)	9	4	3	6	3	4	5	1	2	60	4	0.46
Median PRISM score	15	7	15	13	4	26	23	21	25	28	14	0.0035
Leukocyte count ($\times 10^{-9}$/L)	6.8	18.4	18.8	3.7	15.1	16.1	5.1	35.5	18.1	8.3	9.9	0.6
Platelet count ($\times 10^{-9}$/L)	129	126	123	88	82	111	26	184	91	116	124	0.97
CRP (mmol/L)	52	81	60	138	96	51	78	176	258	105	31	0.44
Lactate (mmol/L)	6.75	0.99	1.71	6.48	0.6	9	5.7	1.7	1.8	9.5	2.2	0.43
Base excess (mmol/L)	1.2	2.4	–8	–15.1	–6.9	–9	–11	–7	–6	–12	–9	0.32
Urea (mmol/L)	11.7	4.9	8	6	3.3	7	7.4	4.4	11.4	7.6	6	0.77
Potassium (mmol/L)	4.5	4.5	4	3.4	3	3	3.7	3.2	3.4	3.2	3.4	0.14
Bilirubin (μmol/L)	12	7	5	3	4	6	9	3	3	12	8	0.78

*A *P* value comparison is shown comparing the Kwan group against the Emonts group, indicating that the two groups have similar demographic characteristics apart from the PRISM score.

CRP, C-reactive protein; DIC, disseminated intravascular coagulation; GpB, Group B Neisseria meningitidis; PCR, polymerase chain reaction; PICU, pediatric intensive care unit; PRISM, Pediatric Risk of Mortality Score.

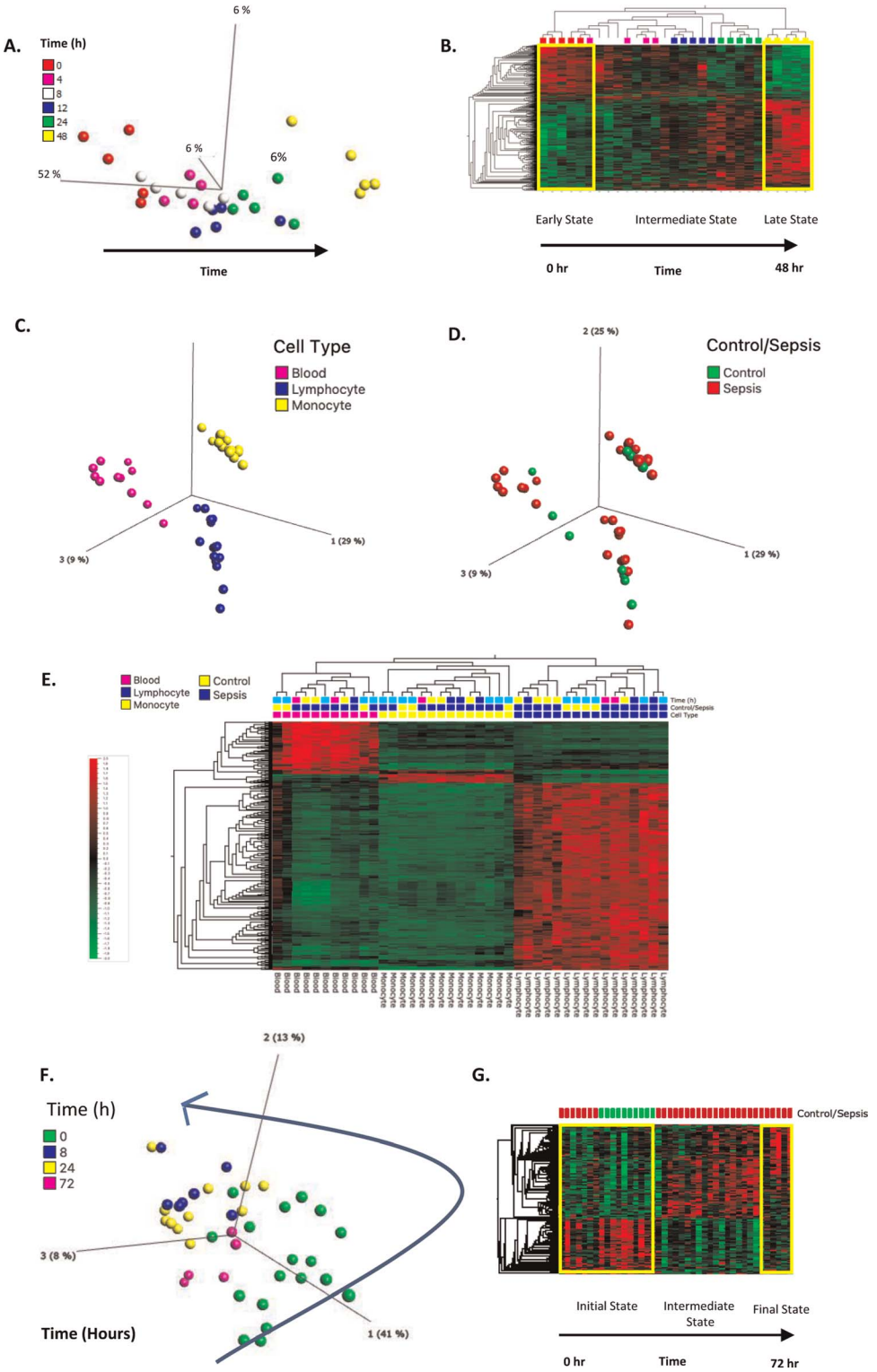

FIG. 2. **Gene expression trajectory from two data series of infants with meningococcal sepsis**. This figure illustrates various analyses conducted on the Kwan (A and B) and Emonts datasets (C–G). In A, a PCA plot of the Kwan dataset using multigroup (ANOVA) temporal analysis ($P \leq 0.01$, 728 genes) shows the expression levels of 728 genes that contribute to differences between time points. Time is identified as the most important component in distinguishing between samples, accounting for 52% of the variation. B presents a synchronized heat map alongside the PCA data for the Kwan dataset, demonstrating the upregulation (red) and downregulation (green) of gene expression. The heat map visualizes gene expression transition from an early to a late state, with significant differences observed between 0 and 48 h. For the Emonts dataset, C shows a PCA plot based on different cell types (blood, lymphocyte, and monocytes) analyzed using ANOVA set to "Time" ($P = 0.01$ and $q = 0.012$), identifying 4,543 significant genes. This dataset also includes a PCA plot comparing controls and sepsis (D) and a corresponding heat map (E). Then, a PCA plot is displayed for the Emonts dataset based on patients and time points, removing the "cell type" factor from the multigroup ANOVA ($P = 0.002$, $q = 0.14$) (F). This PCA plot highlights 776 genes differentially upregulated across time points in the Emonts dataset. At the same time, the associated heat map is presented, showcasing the transition from an early to a late state of sepsis (G).

component, 52%). The heat map (Fig. 2B) synchronized to the Kwan dataset's PCA data showed that most filtered genes exhibited low expression at time 0 that reverted to upregulation by 48 h, demarcating an early, intermediate, and late state. The vertical and horizontal hierarchical clustering heat map indicated that time points 0 and 48 h were the most different in GE and demonstrated the transition from one pattern to another. Similarly, for Emonts data, ANOVA temporal analysis according to different cell types (blood, lymphocytes, and monocytes) generated 4,543 genes of significance ($P = 0.01$ and $q = 0.012$) (Fig. 2, C and D) and sepsis versus controls. In PCA multigroup ANOVA with respect to time (eliminating "cell type"), 776 genes were differentially upregulated across time points (Fig. 2F) ($P = 0.002$, $q = 0.14$, axis 41%, 13%, and 8%) with the associated heat maps (Fig. 2, E and G), showing the transition from an initial state to a final state.

TTCA pathfindR results

Statistically significant differentially expressed genes in the Kwan and Emonts datasets identified by TTCA were enriched according to KEGG pathways and GO-BP terms using the R package Enrichr. The resulting enrichment tables were saved and visualized as bar plots (Fig. 3). KEGG enrichment shows the coronavirus pathway to be enriched for the Kwan dataset (Fig. 3A). Further, for both Kwan and Emonts, neutrophil pathways (mediation, activation, and degradation) are highly enriched. Moreover, both datasets show enrichment for "antigen processing and presentation" and

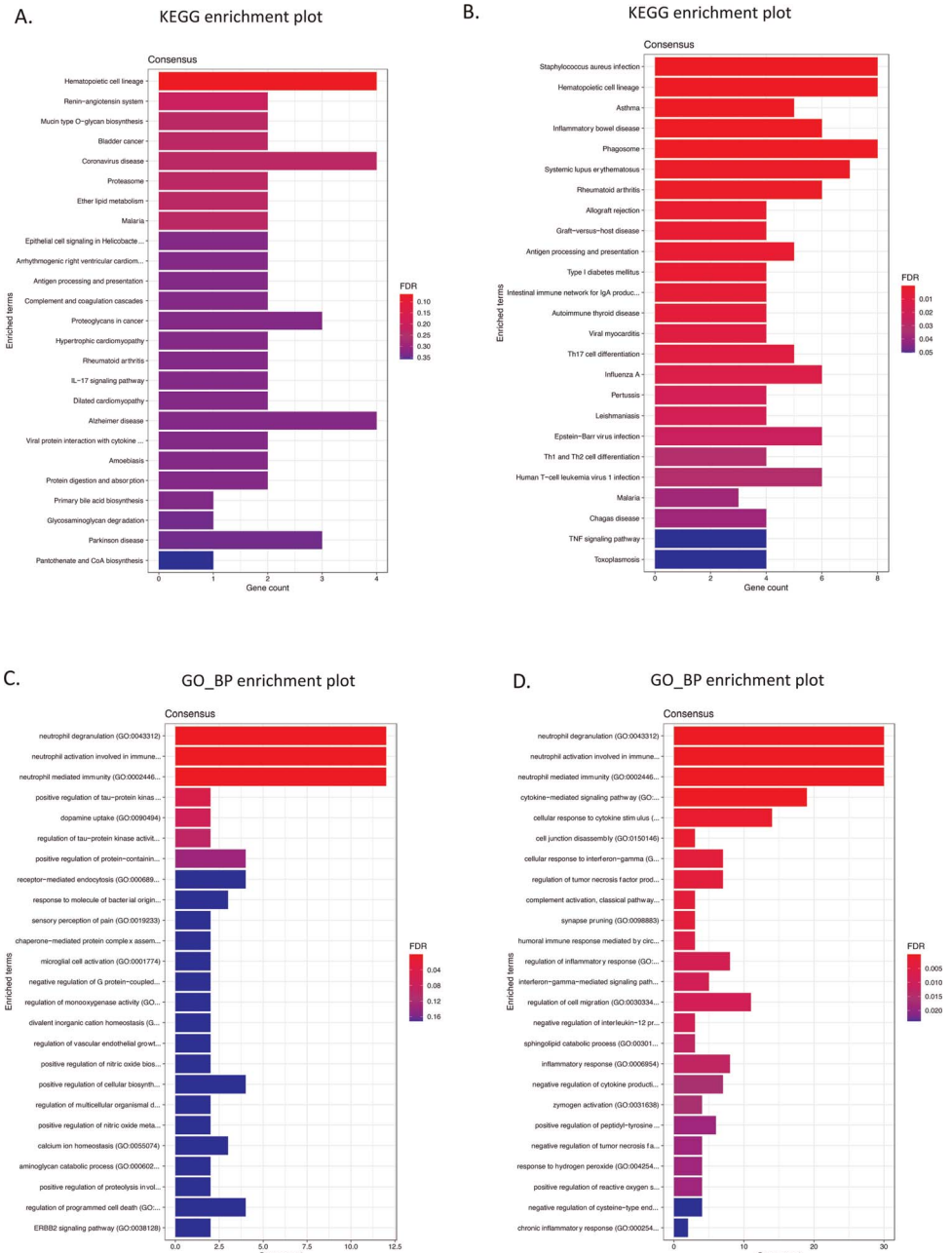

FIG. 3. **Transcript time course analysis (TTCA) for the Kwan and Emonts datasets**. Bar plots are shown, generated from TTCA for the Kwan (A and C) and Emonts (B and D) representing pathway enrichment according to the KEGG database. Also, GO pathways are shown according to biological processes (C and D). The data are scaled in accordance with the false discovery rate. KEGG, Kyoto Encyclopedia of Genes and Genomes.

hematopoietic cell lineage. Emonts datasets showed enrichment for TNF signaling and the regulation of TNF production (Fig. 3, B and D). Both Emonts and Kwan datasets showed GO pathways associated with neutrophil function (Fig. 3, C and D).

The TTCA patterns for VEGF-A and VEGF-B for both Emonts and Kwan datasets suggest a falling trend in GE toward controls, although the trend of VEGF-A in the Emonts dataset was less well defined (Fig. 4).

Curated genes from TTCA were enriched using pathfindR with enrichment charts depicting significant pathways (Fig. 5). For both datasets, KEGG gene enrichment showed pathways related to ribosome and NF-κB signaling pathways. Also, T-helper 17 cell differentiation Kwan (complete response) and Emonts (complete and dynamic response) were enriched. Ribosome gene enrichment was significant for both datasets for complete and dynamic responses. Also, T cell receptor signaling pathways were significant in the complete response for both datasets. Table 3 shows the TTCA gene enrichment comparison of Kwan versus Emonts datasets.

Postmortem sampling GE (GSE141864)

Meningococcal sepsis shock samples were analyzed from postmortem tissue (Fig. 6), with patients with MSS compared against acute noninfectious controls (Fig. 6A). Vascular endothelial growth factor A and NFKB1 were upregulated in patients with MSS compared with controls, whereas VEGF-B was downregulated. Gene expression comparisons across tissues are shown for TNF NFKB1 VEGF-A and VEGF-B patients with MSS (Fig. 6B). Renal VEGF-A was upregulated against all of the other tissue types. Gene expression for liver tissue against other cell types was also compared (not shown) and showed no differentiation for the four gene transcripts studied (NFKB1, TNF, VEGF-A, and VEGF-B). Two-group comparison was undertaken in patients with MSS to compare heart samples against other tissue types (P = 0.001, q = 0.01), with 2,619 genes isolated after filtering (from 26,914 genes) (Fig. 6C). This was then parsed through g:Profiler (settings, organism = *Homo sapiens*, significance threshold = Benjamini-Hochberg FDR, user threshold = 0.05, numeric IDs = ENTREZ_ACC). Then, the 2,619-gene list was also parsed through the ShinyGo platform (version 0.741, setting = *Homo sapiens*), illustrated here (Fig. 6, D–F). Enrichment of pathways related to mitochondrial function was a continuing theme known to be disrupted in MSS. Cardiac muscle enrichment pathways were also noted; cardiac dysfunction is an important feature consistent with severe sepsis and septic shock. Analysis through the Enrichr platform was also undertaken (Fig. 6, G and H), which showed KEGG enrichment for cardiac muscle contraction and oxidative phosphorylation, with Wikipathway gene enrichment for striated muscle contraction and mitochondrial pathways.

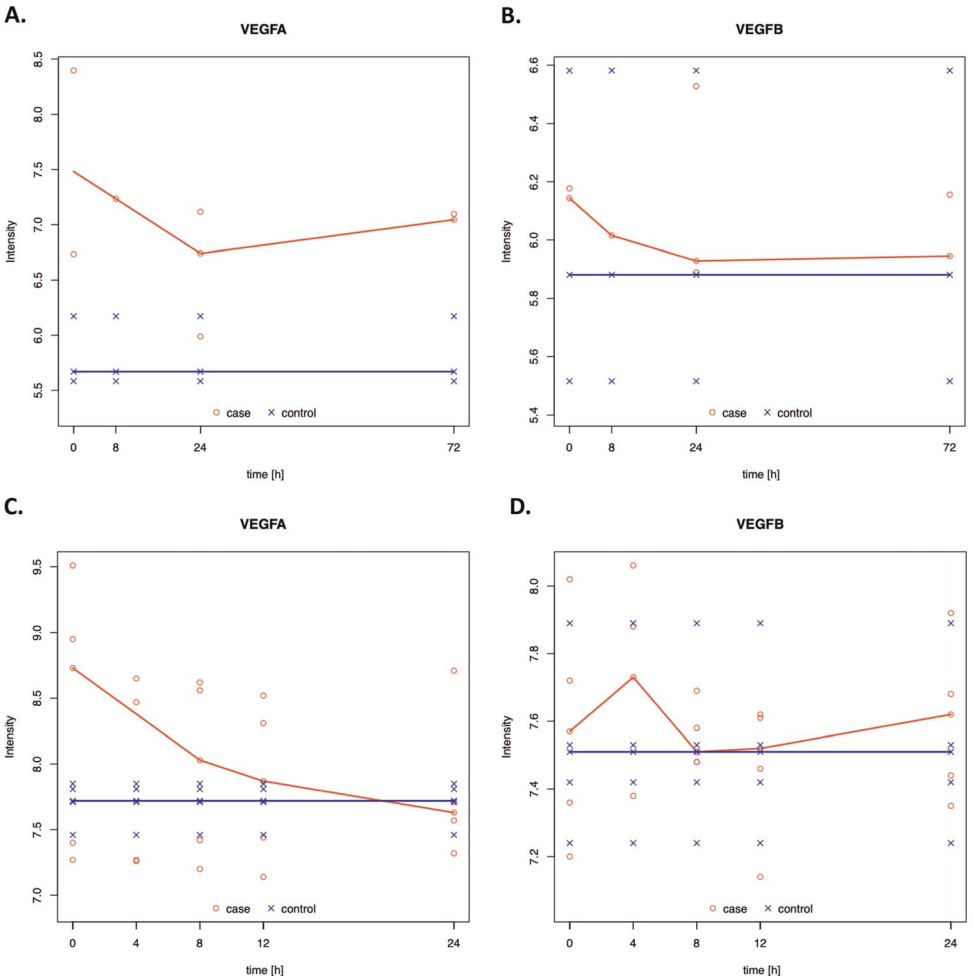

FIG. 4. **Transcript time course analysis (TTCA) for the Kwan and Emonts datasets for VEGF-A and VEGF-B.** TTCA for the Emonts (A and B) and Kwan (C and D) datasets. TTCA gene expression intensities for VEGF-A and VEGF-B showed a tendency toward convergence of cases and controls in both the Emonts and Kwan datasets. VEGF, vascular endothelial growth factor.

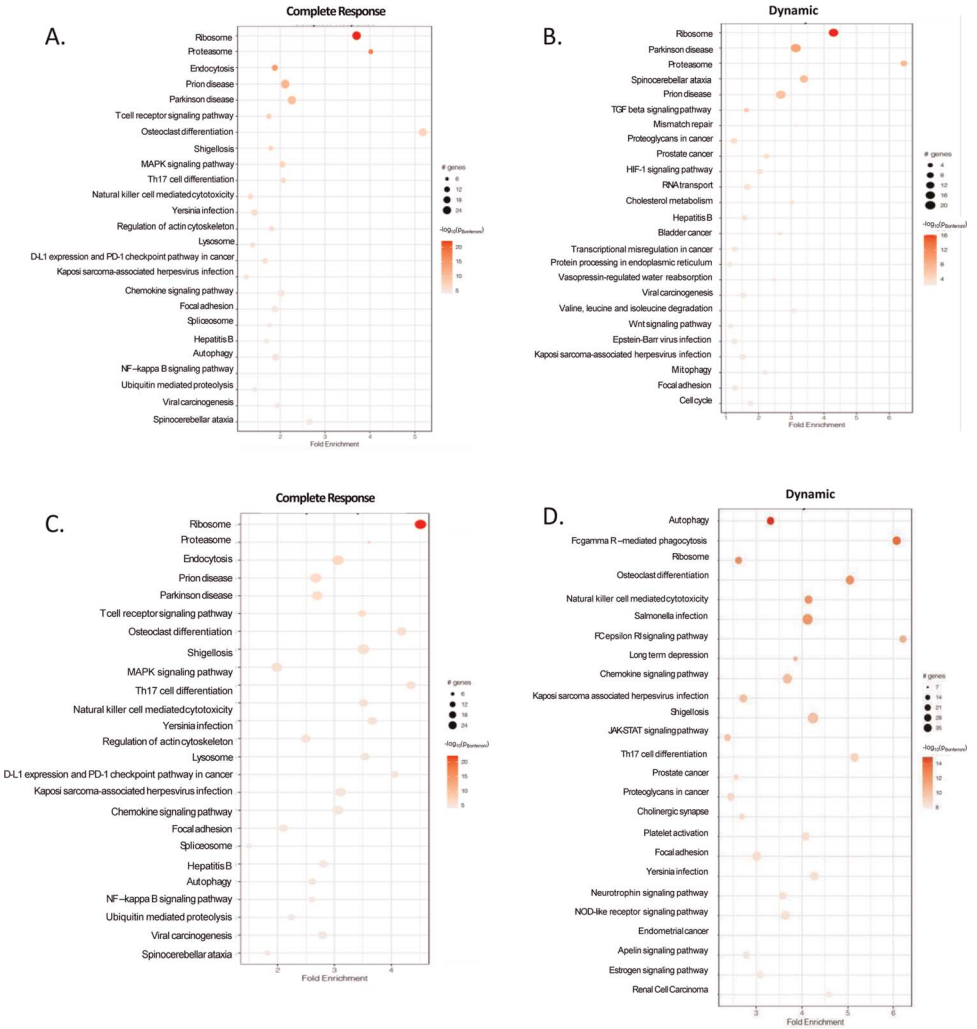

FIG. 5. **pathfindR enrichment analysis of Kwan and Emonts datasets**. From the TTCA data, pathfindR enrichment charts were generated for both the Kwan (A and B) and Emonts datasets (C and D). The data are adjusted in line with the Bonferroni correction.

Also, significant pathways enriched included VEGF-A/VEGF-R, mitogen-activated protein kinase (MAPK), P13k, IL-18, and focal adhesion.

Wright dataset (GSE80496)

Qlucore Omics Explorer was set to the gene symbol setting, and data collapsed by averaging in dataset GSE80496 (Fig. 7).

Box plot analysis showed that, compared with the meningitis group, the MSS group differed the most from the controls (Fig. 7A). In patients with MSS, TNF, NFKB1, and VEGF-A GE were upregulated compared with controls, whereas VEGF-B was downregulated. Patients with MSS were compared with controls after GE filtering ($P = 0.001$ and $q = 0.003$) (Fig. 7B). The subsequent gene list was parsed through g:Profiler generating tree and

TABLE 3. **Curated genes from TTCA gene enrichment for Kwan and Emonts datasets in the "complete response" category**

	Kwan dataset			Emonts		
Gene set	Fold enrichment	*P*	FDR	Fold enrichment	*P*	FDR
KEGG_APOPTOSIS	1.82	0.004	**0.01**	1.69	2.49E-14	**1.50E-13**
KEGG_VEGF_SIGNALING_PATHWAY	0.47	0.931	0.93	1.79	1.11E-12	**3.34E-12**
KEGG_COMPLEMENT_AND_COAGULATION_CASCADES	1.53	0.196	**0.29**	1.36	8.89E-07	**1.78E-06**
Heat shock proteins (HUGO)	1.48	0.173	**0.29**	1.14	8.46E-05	**0.00012693**
Metallothionein genes (HUGO)	0.97	0.656	0.79	0.61	0.831	1.00
Zinc finger genes (HUGO)	1.29	0.003	**0.01**	0.61	0.998	1.00

TTCA and enrichment generated the "complete response" category for the Emonts and the Kwan datasets. The pathway gene sets are compared for each dataset. According to the KEGG apoptosis pathway, genes are enriched for apoptosis in both datasets. The zinc finger genes are enriched for Kwan, whereas there was no enrichment for the Emonts dataset. For Emonts VEGF, complement and coagulation cascades and heat shock proteins are also noted.

FDR, false discovery rate; KEGG, Kyoto Encyclopedia of Genes and Genomes; TTCA, transcript time course analysis; VEGF, vascular endothelial growth factor.

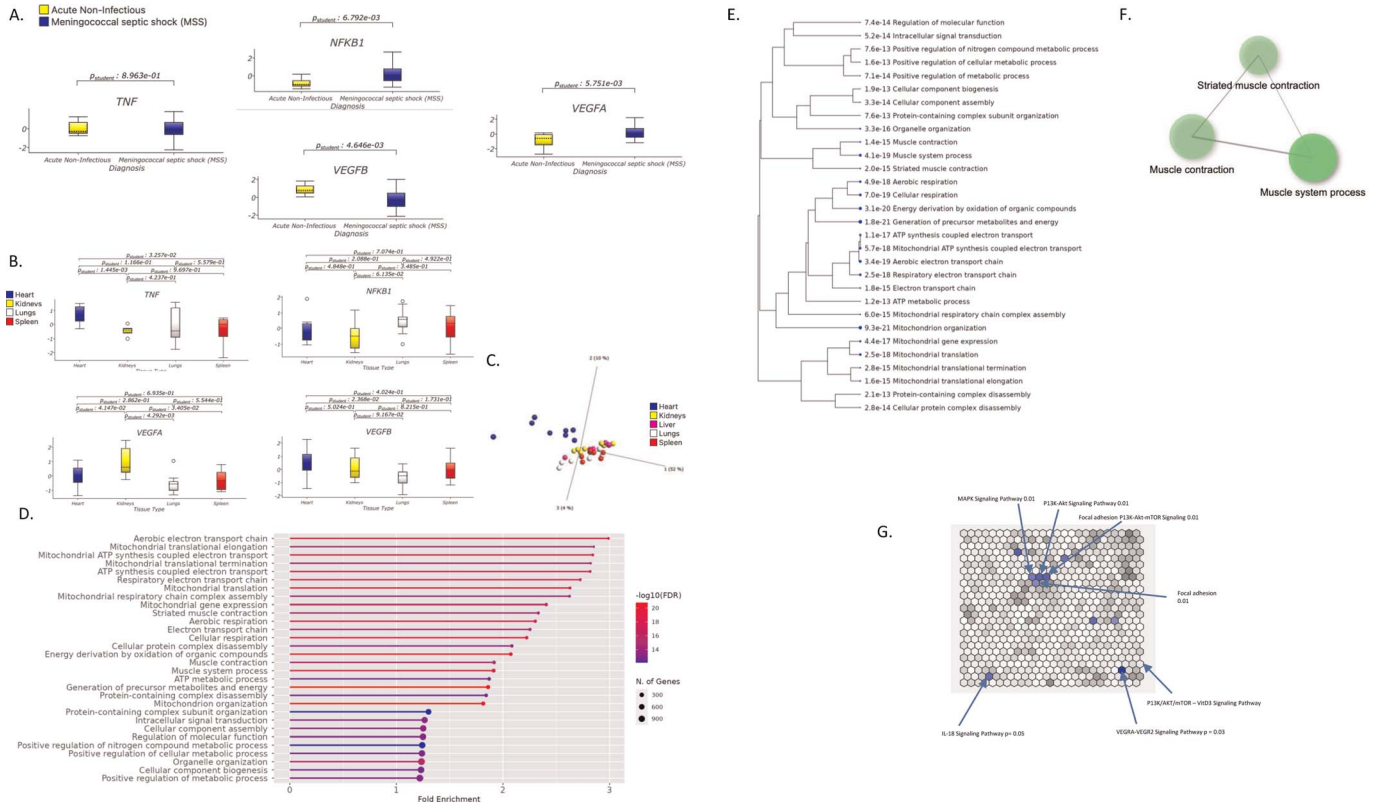

FIG. 6. **Transcriptional changes in postmortem samples in *Neisseria* meningococcal sepsis *versus* controls**. This figure represents an analysis of the postmortem dataset GSE141864, comparing individuals with noninfectious causes for death (controls) and patients diagnosed with *Neisseria* meningococcal septic shock (MSS). The data in A was organized based on gene symbol, and box plot analysis was conducted. In MSS cases, there was a significant upregulation of NFKB1 and VEGF-A GE compared with controls, whereas VEGF-B was downregulated. However, there was no difference in TNF GE between cases and controls. GE was used to analyze tissue from patients with MSS (B). TNF GE showed the highest upregulation in the heart compared with the kidneys and spleen, with no difference compared with the lungs. No significant differential GE was noted for NFKB1 across tissue types. In the kidneys, VEGF-A exhibited upregulation compared with the heart, lungs, and spleen, whereas VEGF-B showed upregulation in the heart compared with the lungs. A two-group comparison was performed between heart tissue and all other tissues using QOE ($P = 0.01$ and $q = 0.05$). This analysis filtered 26,193 variables to 6,179 genes and generated a three-axis principal component analysis plot (C). The resulting differential gene set was then analyzed using the ShinyGo platform generating lollipop and tree plots (D and E). The ShinyGO platform was set for *Homo sapiens* and an FDR cutoff of 0.05 to display the top 30 pathways. The lollipop and tree plots depicted various aspects of the respiratory chain, aerobic respiration, and mitochondrial function pathways. A network plot was also generated from the gene 6,179 list, revealing networks associated with the heart muscle (F). A subset of 19 genes was removed from the gene list to comply with the Enrichr platform, resulting in 6,160 enriched genes showing enrichment by hexagon plots (G). Highly significant pathways included VEGF-A/VEGF-R, MAPK, P13k-Akt, IL-18, and focal adhesion. FDR, false discovery rate; GE, gene expression; NFKB1, NF-κB1; QOE, Qlucore Omics Explorer; VEGF, vascular endothelial growth factor; VEGF, VEGF receptor.

lollipop plots (Fig. 7, C and D). Further, the gene list underwent analysis by Enrichr generating bar and hexagon plots (Fig. 7, E and F). Cytoplasmic ribosomal proteins were noted to be significantly enriched. Further significant pathways related to MAPK, P13K-Akt, VEGF-A, IL-4, epidermal growth factor/epidermal growth factor receptor, and IL-18 were noted.

Four gene transcript patterns (VEGF-A, VEGF-B, TNF, and NFKB1 GE in temporal datasets

In the Emonts dataset, on analysis according to cell type, NFKB1 differentiated all three categories (blood, lymphocytes, and monocytes) (Fig. 8A). At the same time, blood and monocytes showed VEGF-A upregulation and VEGF-B downregulation compared with lymphocytes. For Emonts, when controls were compared against sepsis patients, TNF, NFKB1, and VEGF-A were upregulated against controls, with no change noted in VEGF-B (Fig. 8B). Of the four GE transcripts under study, for Emonts and Kwan, the only gene to show a temporal difference was NFKB1 (Fig. 8, C and D).

For the Wong dataset, septic shock D3, compared with controls D3, was upregulated for NFKB1 and VEGF-A and downregulated for VEGF-B (Fig. 8E). This was also similar for sepsis D3 versus controls D3. For SIRS D3 versus controls D3, NFKB1 only was upregulated, whereas VEGF-B was downregulated (Fig. 8E). Gene set expression analysis was performed for the genes of interest in the Wong dataset; septic shock D3 versus controls is illustrated (Fig. 8F), and all of the combinatory GSEA comparisons are listed (Table 4), with the KEGG VEGF signaling pathway enrichment being noteworthy for the sepsis but not for the SIRS categories.

DISCUSSION

The primary aim of this study was to enhance our understanding of dynamic changes associated with sepsis from a transcriptomic perspective. Thus, using a systemic search strategy, we found relevant temporal and cross-sectional datasets for childhood sepsis

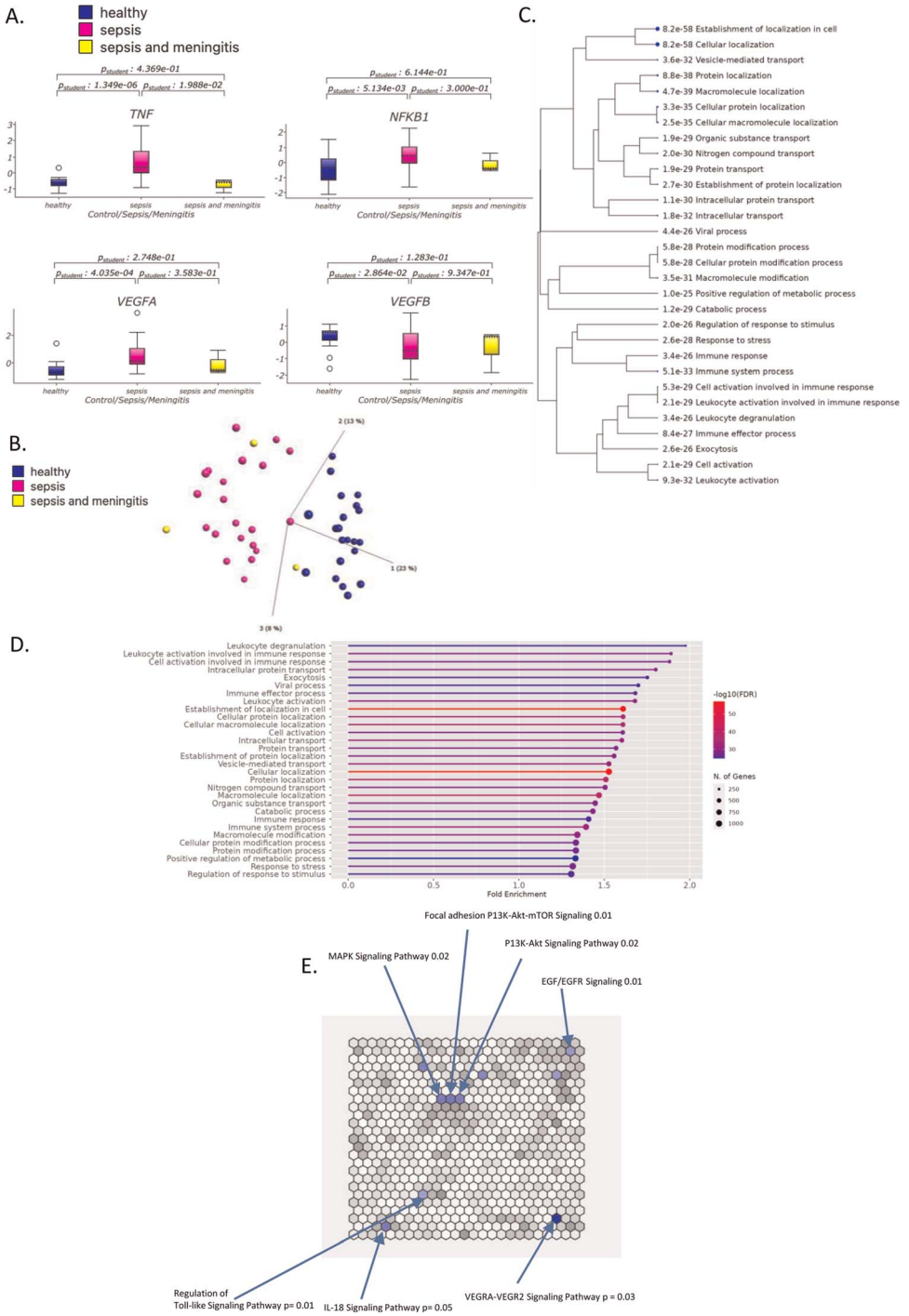

FIG. 7. **Transcript (cross-sectional) of the Wright dataset**. The GSE80496 *Neisseria* meningococcal dataset was classified into healthy (controls, n = 21) and meningococcal disease (sepsis only, n = 21; sepsis with meningitis, n = 3) groups. Box plot analysis (A) showed elevated GE in patients with sepsis alone compared with both controls and patients with sepsis and meningitis. Specifically, NFKB1 and VEGF-A GE are elevated in patients with sepsis only, compared with controls, whereas VEGF-B GE is downregulated. GSE80496 dataset contains 18,631 variables when averaged according to gene symbol. Principal component analysis plot is illustrated (B). This dataset is then filtered in QOE ($P = 0.001$ and $q = 0.003$), leading to 5,596 unique genes, which are then parsed through the ShinyGO platform (setting = *Homo sapiens*, FDR cutoff = 0.05, top pathways shown =30, database used = GO biological process). This results in the tree diagram (C) and lollipop plot shown (D). Also, the same gene list is pasted into the Enrichr tool, generating enriched pathways in the KEGG 2021 database category. These data are sent through an Appyter connection to generate a hexagon plot (E). The hexagonal canvas plot shows terms from the WikiPathway 2021 Human gene set library. Each hexagon in the plot represents a single term. The brighter the color, the higher the Jacquard similarity between the term gene set and the input gene set. Terms highlighted in blue show the most significant overlap with the input query gene set, with similar gene sets grouped close to each other. FDR, false discovery rate; GE, gene expression; KEGG, Kyoto Encyclopedia of Genes and Genomes; QOE, Qlucore Omics Explorer; VEGF, vascular endothelial growth factor.

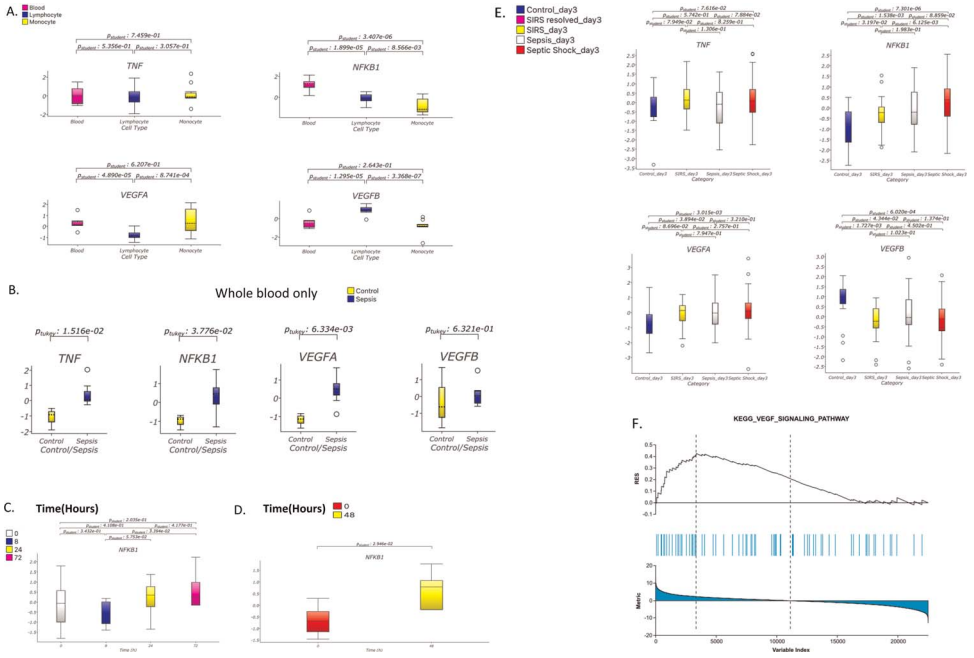

FIG. 8. **Comparing proinflammatory gene expression transcripts in meningococcal and polymicrobial sepsis and VEGF-B GE**. This figure compares GE across *Neisseria* meningococcal and polymicrobial sepsis. The figure includes A, B, and C (Emonts dataset); D (Kwan dataset); and E (Wong dataset). A displays GE analysis according to the cell type in the Emonts dataset, specifically for TNF, NFKB1, VEGF-A, and VEGF-B genes, with controls removed and gene symbols collapsed. B analyzes the same genes for the Emonts dataset, focusing on GE in whole blood and comparing sepsis patients against controls. Among the four selected genes, only NFKB1 is depicted in a box plot, illustrating temporal changes in GE for the Emonts (C) and Kwan (D) datasets, with controls removed for the Emonts dataset. The NFKB1 gene shows a temporal increase in expression for the Emonts dataset when comparing 8 h with 72 h, whereas no difference is observed across the start and end points. In the Kwan dataset, there is also an increase in NFKB GE between the 0- and 48-h time points. The Wong dataset (GSE13904), including controls, is analyzed in E. Using the VEGF.gmt file, GSEA is performed using a two-group comparison of septic shock day 3 versus controls day 3, with 124 samples and 22,480. F presents the GSEA result, indicating enrichment for the KEGG VEGF signaling pathway (Net enrichment score = 1.57, $P = 0.04$, and $q = 0.17$) in the septic shock day 3 versus controls day 3 comparison. GE, gene expression; GSEA, gene set expression analysis; KEGG, Kyoto Encyclopedia of Genes and Genomes; NFKB1, NF-κB1; VEGF, vascular endothelial growth factor.

from the clinical literature; four were related to *Neisseria* meningococcal disease and one to polymicrobial sepsis. Two time-series meningococcal datasets (Kwan and Emonts) suggested temporal organization, with PCA heat maps showing three phases (early, intermediate, and late). Transcript time course analysis allows the appreciation of dynamic changes in GE and was thus applied to our work. Although there were potential similarities in the Emonts and Kwan trajectories using TTCA, this was difficult to compare because of the different periods of the two independent studies. Transcript time course analysis provided a temporal illustration of GE and was combined with Pearson correlation and pathR enrichment analysis mapped to the KEGG database. Using TTCA applied to the *Neisseria* meningococcal disease temporal datasets (Kwan and Emonts), gene enrichment pathways related to coronavirus infection were identified, suggesting the sharing of pathways related to disease pathogenesis for both MSS and severe acute respiratory syndrome.

Gene set expression analysis is a method allowing the comparison of multiple gene sets or pathways and was used by Raman et al. (38) on the Kwan dataset to show a temporal fall in oxidative phosphorylation GE. Our study also used GSEA applied to the polymicrobial dataset, using controls as a comparison, to

TABLE 4. **GSEA comparison against day 3 controls in the Wong (polymicrobial sepsis) dataset**

Gene set	Keyword	No. gene sets downloaded	Septic shock day 3 vs. control day 3			Sepsis day 3 vs. control day 3			SIRS day 3 vs. control day 3			SIRS resolved day 3 vs. control day 3		
			NES	*P*	*q*	NES	*P*	*q*	NES	*P*	*q*	NES	*P*	*q*
KEGG VEGF signaling pathway	VEGF	20	1.57	0.04	0.17	1.56	0.03	0.16	NS	NS	NS	NS	NS	NS
Hallmark TNFA signaling *via* NFKB	NFKB1	746	1.64	0.05	0.18	NS	NS	NS	NS	NS	NS	NS	NS	NS
Hallmark inflammatory response	NFKB1	746	1.79	0.02	0.11	1.73	0.03	0.14	NS	NS	NS	NS	NS	NS
GOBP Response to IL-6	NFKB1	746	1.79	0.004	0.1	1.98	0	0.02	NS	NS	NS	NS	NS	NS
GOBP TNF superfamily cytokine production	TNF	1,329	1.7	0.02	0.13	1.8	0.02	0.06	NS	NS	NS	1.64	0.04	0.15
GOBP TNF-mediated signaling pathway	TNF	1,329	NS	NS	NS	NS	NS	NS	NS	NS	NS	NS	NS	NS

Using GSEA, a two-group comparison was undertaken against day 3 controls according to the first row, with the GSEA label set to "Category" for the two-group comparison. The headline gene sets are shown (first column), consisting of a number of reference gene sets downloaded from MSigDB according to the keyword (second column). The number of gene sets downloaded per keyword is shown (third column). Significant gene sets are shown in the table according to $P < 0.05$ and $q < 0.25$, with their corresponding NES.

GSEA, gene set expression analysis; KEGG, Kyoto Encyclopedia of Genes and Genomes; NES, net enrichment score; NS, Not Significant; NFKB1, NF-κB1; SIRS, systemic inflammatory response syndrome; VEGF, vascular endothelial growth factor.

differentiate between the SIRS and sepsis. Sepsis showed significant enrichment for VEGF signaling, IL-6 response, TNF signaling *via* NFKB, inflammatory response, and TNF superfamily cytokine production. In contrast, the SIRS group showed no differential enrichment of the aforesaid pathways. Further, GSEA showed the enrichment of the TNF superfamily cytokine production gene set in septic shock and sepsis patients (compared with controls). However, GSEA suggested that the TNF-mediated signaling pathway was no different in sepsis, SIRS, and controls groups. One explanation for TNF superfamily production being significant but lacking TNF-mediated signaling could be as a manifestation of sepsis-associated dysfunction. Gene set expression analysis was shown to differentiate patients with sepsis from those with SIRS. Therefore, GSEA may have utility in a predictive capacity, such as demonstrated through GSEA-based modular cluster analysis, which has helped to identify early predictive biomarkers of sepsis (39,40), relating changes to outcomes by Kaplan-Meier analysis (41).

Given the proinflammatory nature of sepsis, three genes with corresponding proinflammatory proteins were chosen for analysis (VEGF-A, TNF, and NFKB1). TNF GE was differential only in the Wright dataset, showing gene upregulation in children with MSS against controls and when children with sepsis were compared with those with combined sepsis and meningitis. From whole blood, the Emonts dataset showed all three genes upregulated in patients with MSS versus controls. However, from a temporal perspective, only NFKB1 elicited a temporal relationship in both Emonts and Kwan. Further, the Emonts study allowed a comparison of GE according to cell category (whole blood, lymphocytes, and monocytes), illustrating that NFKB1 GE can differentiate by cell type. In the Wright and Brusletto datasets, NFKB1 genes were upregulated in MSS versus control patients. Further, NFKB1 was upregulated in the Wong dataset compared with controls for both septic shock and sepsis groups. Several studies have identified the NF-κB as the primary signaling pathway for the proinflammatory cytokine/chemokine response induced by severe acute respiratory syndrome coronavirus 2 infection (42). We concentrated on NFKB1 GE as the corresponding protein forms a subunit with RelA regulating GE involved in immune and inflammatory responses. NFKB1/RelA complex contributes to the predominant NF-κB transcriptional activity through proinflammatory mediation (43). AbdAllah et al. (44) also demonstrated the importance of NF-κB in sepsis by examining the Toll-like receptor pathway in a case-control study of neonates with sepsis. Based on a receiver operating characteristic curve, NFKB1 transcript levels showed good sepsis biomarking potential and were gender independent. Moreover, Liu et al. (45) examined transcription factor genes in adults with sepsis, showing protein-protein interaction for NFKB1 being present at the center of the networks, with the potential role also in cytokine-mediated signaling and cell communication. Studies suggest that NF-κB inhibitors may offer useful therapies for sepsis, underlying the importance of the NF-κB pathway (46). Given the changes in NFKB1 GE noted in our study across sepsis datasets, NFKB1 requires further scientific consideration in its role as a temporal biomarker and in the value of NFKB1 inhibition. Inhibition of NF-κB activation, resulting in decreased proinflammatory cytokine generation and the restriction of the inflammatory response, could also have therapeutic value.

The Brusletto and Wright datasets show pathway enrichment for VEGFRA-VEGFR2 signaling and P13K/AKT/mTOR. Further, in the Kwan and Emonts datasets, KEGG VEGF signaling enrichment was noted by TTCA. Also in the Wong dataset, septic shock D3 and sepsis D3, versus controls D3 showed KEGG VEGF signaling pathway enrichment. This consistent pattern of enrichment underlines the importance of VEGF and its associated pathway. Vascular endothelial growth factor A activates both the MAPK and phosphatidylinositol-3-kinase-Akt (PI3K-Akt) signaling pathways critical for cellular development, proliferation, and survival (47,48). In addition, VEGF-A stimulates the activation of diverse signaling proteins in endothelial cells, such as the mammalian target of rapamycin (mTOR) (49). This serine/threonine kinase divides into two complexes called mTORC1 and mTORC2, resulting in downstream PI3K-Akt-mTOR modulation of angiogenesis. Thus, MAPK, PI3K-Akt, and mTOR are activated by VEGF-A to influence angiogenesis. Accordingly, we investigated VEGF-A GE in the sepsis GE datasets. The dynamics of the interaction of VEGF-A and VEGF-B in sepsis have not been previously described. In the Brusletto dataset postmortem kidney tissue, VEGF-A GE was upregulated against all other tissue types and VEGF-B downregulated. The Brusletto dataset is unique in allowing a view of end-stage disease from postmortem tissue data, suggesting an end-point interpretation of the GE trajectory. In the Wright datasets, VEGF-A showed gene upregulated in patients with MSS versus controls, with VEGF-B showing downregulation. Vascular endothelial growth factor A likely has an intricate molecular relationship with VEGF-B because both activate the VEGF-R1 receptor. However, the relationship between VEGF-A and VEGF-B has not been previously investigated in sepsis. In the Brusletto, Wright, and Wong datasets, VEGF-A was upregulated in combination with VEGF-B downregulation in children with sepsis against controls. However, in the Emonts dataset, although VEGF-A was upregulated in MSS versus controls, there was no change for VEGF-B GE. Moreover, when the Emonts dataset was analyzed according to cell type, VEGF-A was upregulated and VEGF-B downregulated for whole blood and monocytes compared with lymphocytes. The significance of this pattern of VEGF-A and VEGF-B GE across independent studies may be related to the differential function of the corresponding proteins. Vascular endothelial growth factor B has approximately 47% amino acid sequence identical to VEGF-A with differential effects (50). The most popular and thoroughly researched VEGF subtype, VEGF-A, has been linked to numerous physiological and pathological processes, including angiogenesis, wound healing, and tumor formation. On the other hand, VEGF-B has been implicated in other processes, such as cardioprotection and metabolic regulation, and is less powerful in inducing angiogenesis. Vascular endothelial growth factor A and VEGF-B are members of the VEGF protein family regulating angiogenesis (51). This study intimates the importance of VEGF-A GE because of its acute rise in sepsis and its role in proinflammation, although the fall in VEGF-B GE requires further study. Future research should consider VEGF-A and VEGF-B interactions, given the potential reciprocal pattern of changes in acute sepsis.

The analysis of temporal GE in sepsis was central to this study. However, it was limited by the availability of only two temporal

datasets (Kwan and Emonts) in the clinical literature, which used a multisampling strategy in pediatric sepsis within the first 1 to 2 days of PICU admission. The Kwan dataset lacked healthy controls, whereas the Emonts dataset included age- and gender-matched controls, possibly preventing the matching of these datasets. The inclusion of controls is also desirable for TTCA. The Brusletto dataset provided controls for comparison against children with MSS, although these controls were derived from adult samples. A further limitation was the small sample sizes in the Kwan and Emonts datasets, which posed a statistical challenge. A supervised strategy was used to structure differential GE analysis of TNF, NF-κB, and VEGF-A differential GE. However, unsupervised analysis of transcriptomic data was also adopted using TTCA. This revealed TNF and NF-κB signaling pathways to be enriched in the Kwan and Emonts datasets. Further, using TTCA applied to the polymicrobial dataset showed evidence of TNFA signaling and the VEGF pathway (septic shock D3 samples com-pared against controls D3). Furthermore, Emonts also demonstrated VEGF pathway enrichment by TTCA. Moreover, when genes differentially expressed in myocardium tissue were compared against other tissues (using Enrichr), the Brusletto dataset showed enrichment for VEGF-A/VEGF-R2 signaling. Vascular endothelial growth factor is a key regulator of angiogenesis, and VEGF-R2 is a receptor for VEGF-A. The observed enrichment for VEGF-A/VEGF-R2 signaling indicates that this pathway may play a critical role in the myocardium, thus providing grounds for future downstream analysis using the genes discussed in this article. In summary, we believe future work should include temporal transcriptomic studies with larger datasets and relevant controls and the use of the gene combination adopted in this article.

The proinflammatory pattern of GE, as intimated by changes in TNF, NFKB1, and VEGF-A explored in this article, follows our work in Kawasaki disease, which also demonstrated similar changes in VEGF-A and VEGF-B GE. Given the acute elevation of VEGF-A GE noted in sepsis studies, especially with respect to postmortem renal tissue, future work should consider the value of VEGF-A counteraction in sepsis. The importance of VEGF-A is evident in murine studies where myeloid-specific St18-deficient mice exhibit enhanced serum VEGF-A concentration (52), leading to a higher risk of colitis, LPS-induced shock, and polymicrobial sepsis. Axitinib-induced VEGF signaling inhibition improved survival rates in these mice, suggesting mortality improvement by countering VEGF-A's inflammatory effect. Furthermore, understanding changes in VEGF-B relative to VEGF-A and the resulting therapeutic insights could provide unique insights for future research.

CONCLUSION

This study demonstrated temporal changes in acute sepsis. Unsupervised heat plots revealed distinct early, intermediate, and late phases of MSS based on GE analysis. Consistent upregulation of VEGF-A and NFKB1 in sepsis GE datasets was observed. The application of TTCA to temporal datasets indicated potential enrichment of coronavirus pathways, suggesting possible overlap with sepsis processes. Notably, temporal changes in NFKB1 GE were identified in the MSS datasets, suggesting its potential as a biomarker for future analysis. The study also emphasized the significance of VEGF-A upregulation in acute sepsis.

Furthermore, given the limited scientific knowledge surrounding the role of VEGF-B in sepsis, its close molecular similarity to VEGF-A in terms of structure and receptor binding makes it an area of scientific interest. The study suggests that investigating both proteins in combination could provide valuable insights. Overall, the importance of comprehending the temporal dynamics of sepsis from a transcriptomic perspective was highlighted. Suggestions for future research include exploring biomarkers such as NFKB1, investigating VEGF-A inhibition, and examining the combined role of VEGF-A and VEGF-B in sepsis.

A video summary of the article is provided (http://links.lww.com/SHK/B770).

ACKNOWLEDGMENTS

The authors thank the anonymous reviewers for their insightful comments and suggestions. They also thank Dr. David Inwald, PICU Addenbrookes Hospital, Cambridge, for reading and providing feedback on the article; his contribution to the field of genomics is immense and irreplaceable. ZH acknowledges the support of the UK Engineering and Physical Sciences Research Council: grants Ref. EP/M026981/1, EP/T021063/1, EP/T024917/1. Finally, and certainly, not least, they thank Prof. Hector Wong, whose decades-long contribution to the genomics of sepsis remains an enduring legacy.

REFERENCES

1. Rudd KE, Johnson SC, Agesa KM, et al. Global, regional, and national sepsis incidence and mortality, 1990–2017: analysis for the global burden of disease study. *Lancet*. 2020;395(10219):200–211.
2. Larsen GY, Brilli R, Macias CG, et al. Development of a quality improvement learning collaborative to improve pediatric sepsis outcomes. *Pediatrics*. 2021; 147(1):e20201434.
3. Fleischmann-Struzek C, Goldfarb DM, Schlattmann P, et al. The global burden of paediatric and neonatal sepsis: a systematic review. *Lancet Respir Med*. 2018; 6(3):223–230.
4. Gotmaker R, Peake SL, Forbes A, et al, ARISE Investigators. Mortality is greater in septic patients with hyperlactatemia than with refractory hypotension. *Shock*. 2017; 48(3):294–300.
5. Guest RL, Rutherford ST, Silhavy TJ. Border control: regulating LPS biogenesis. *Trends Microbiol*. 2021;29(4):334–345.
6. Garcia-Vello P, Di Lorenzo F, Zucchetta D, et al. Lipopolysaccharide lipid A: a promising molecule for new immunity-based therapies and antibiotics. *Pharmacol Ther*. 2022;230:107970.
7. Rashid A, Anwary AR, Al-Obeidat F, et al. Application of a gene modular approach for clinical phenotype genotype association and sepsis prediction using machine learning in meningococcal sepsis. *Inform Med Unlocked*. 2023;101293.
8. Liu T, Zhang L, Joo D, et al. NF-κB signaling in inflammation. *Signal Transduct Target Ther*. 2017;2:17023.
9. Dabravolski SA, Khotina VA, Omelchenko AV, et al. The role of the VEGF family in atherosclerosis development and its potential as treatment targets. *Int J Mol Sci*. 2022;23(2):931.
10. Gorenjak V, Vance DR, Petrelis AM, et al. Peripheral blood mononuclear cells extracts VEGF protein levels and VEGF mRNA: associations with inflammatory molecules in a healthy population. *PloS One*. 2019;14(8):e0220902.
11. Salven P, Hattori K, Heissig B, et al. Interleukin-1alpha promotes angiogenesis *in vivo via* VEGFR-2 pathway by inducing inflammatory cell VEGF synthesis and secretion. *FASEB J*. 2002;16(11):1471–1473.
12. De Palma M. Partners in crime: VEGF and IL-4 conscript tumour-promoting macrophages. *J Pathol*. 2012;227(1):4–7.
13. Loeffler S, Fayard B, Weis J, et al. Interleukin-6 induces transcriptional activation of vascular endothelial growth factor (VEGF) in astrocytes *in vivo* and regulates VEGF promoter activity in glioblastoma cells *via* direct interaction between STAT3 and Sp1. *Int J Cancer*. 2005;115(2):202–213.
14. Jing Y, Ding M, Fu J, et al. Neutrophil extracellular trap from Kawasaki disease alter the biologic responses of PBMC. *Biosci Rep*. 2020;40(9):BSR20200928.
15. Lv YW, Wang J, Sun L, et al. Understanding the pathogenesis of Kawasaki disease by network and pathway analysis. *Comput Math Methods Med*. 2013;2013:989307.
16. Wang Y, Yang C. Enhanced VEGF-A expression and mediated angiogenic differentiation in human gingival fibroblasts by stimulating with TNF-α *in vitro*. *J Dent Sci*. 2022;17(2):876–881.

17. Yano K, Liaw PC, Mullington JM, et al. Vascular endothelial growth factor is an important determinant of sepsis morbidity and mortality. *J Exp Med*. 2006;203(6): 1447–1458.
18. Shibuya M. VEGF-VEGFR system as a target for suppressing inflammation and other diseases. *Endocr Metab Immune Disord Drug Targets*. 2015;15(2):135–144.
19. Zhang F, Tang Z, Hou X, et al. VEGF-B is dispensable for blood vessel growth but critical for their survival, and VEGF-B targeting inhibits pathological angiogenesis. *Proc Natl Acad Sci*. 2009;106(15):6152–6157.
20. Räsänen M, Degerman J, Nissinen TA, et al. VEGF-B gene therapy inhibits doxorubicin-induced cardiotoxicity by endothelial protection. *Proc Natl Acad Sci*. 2016; 113(46):13144–13149.
21. Li X, Lee C, Tang Z, et al. VEGF-B: a survival, or an angiogenic factor? *Cell Adh Migr*. 2009;3(4):322–327.
22. Rashid A, Toufiq M, Khilnani P, et al. VEGF subtype A and B gene expression, clues to a temporal signature in Kawasaki disease, implications for coronary pathogenesis through a secondary analysis of clinical datasets. *medRxiv*. 2022;2022.2008. 2008.22278559.
23. Barrett T, Edgar R. Mining microarray data at NCBI's Gene Expression Omnibus (GEO)*. *Methods Mol Biol*. 2006;338:175–190.
24. Kwan A, Hubank M, Rashid A, et al. Transcriptional instability during evolving sepsis may limit biomarker based risk stratification. *PloS One*. 2013;8(3):e60501.
25. Herberg JA, Kaforou M, Wright VJ, et al. Diagnostic test accuracy of a 2-transcript host RNA signature for discriminating bacterial vs viral infection in febrile children. *JAMA*. 2016;316(8):835–845.
26. Brusletto BS, Løberg EM, Hellerud BC, et al. Extensive changes in transcriptomic "fingerprints" and immunological cells in the large organs of patients dying of acute septic shock and multiple organ failure caused by *Neisseria meningitidis*. *Front Cell Infect Microbiol*. 2020;10:42.
27. Wong HR, Cvijanovich N, Allen GL, et al. Genomic expression profiling across the pediatric systemic inflammatory response syndrome, sepsis, and septic shock spectrum. *Crit Care Med*. 2009;37(5):1558–1566.
28. Emonts Marieke MDR, Schonewille T, Hazelzet JA, et al. Gene expression profiling in pediatric meningococcal sepsis reveals dynamic changes in NK-cell and cytotoxic molecules. *Cite Seer X*. 2008.
29. Subramanian A, Tamayo P, Mootha VK, et al. Gene set enrichment analysis: a knowledge-based approach for interpreting genome-wide expression profiles. *Proc Natl Acad Sci U S A*. 2005;102(43):15545–15550.
30. Ge SX, Jung D, Yao R. ShinyGO: a graphical gene-set enrichment tool for animals and plants. *Bioinformatics*. 2020;36(8):2628–2629.
31. Reimand J, Arak T, Adler P, et al. g:Profiler—a web server for functional interpretation of gene lists (2016 update). *Nucleic Acids Res*. 2016;44(W1):W83–W89.
32. Albrecht M, Stichel D, Muller B, et al. TTCA: an R package for the identification of differentially expressed genes in time course microarray data. *BMC Bioinform*. 2017;18(1):33.
33. Adler P, Reimand J, Janes J, et al. KEGGanim: pathway animations for high-throughput data. *Bioinformatics*. 2008;24(4):588–590.
34. Eyre TA, Ducluzeau F, Sneddon TP, et al. The HUGO gene nomenclature database, 2006 updates. *Nucleic Acids Res*. 2006;34(Database Issue):D319–D321.
35. Ulgen E, Ozisik O, Sezerman OU. pathfindR: an R package for comprehensive identification of enriched pathways in omics data through active subnetworks. *Front Genet*. 2019;10:858.
36. Huntley RP, Sawford T, Mutowo-Meullenet P, et al. The GOA database: Gene Ontology annotation updates for 2015. *Nucleic Acids Res*. 2015;43(D1):D1057–D1063.
37. Kuleshov MV, Jones MR, Rouillard AD, et al. Enrichr: a comprehensive gene set enrichment analysis web server 2016 update. *Nucleic Acids Res*. 2016;44(W1): W90–W97.
38. Raman S, Klein N, Kwan A, et al. Oxidative phosphorylation gene expression falls at onset and throughout the development of meningococcal sepsis-induced multiorgan failure in children. *Intensive Care Med*. 2015;41(8):1489–1490.
39. Li Z, Huang B, Yi W, et al. Identification of potential early diagnostic biomarkers of sepsis. *J Inflamm Res*. 2021;14:621–631.
40. Zeng X, Feng J, Yang Y, et al. Screening of key genes of sepsis and septic shock using bioinformatics analysis. *J Inflamm Res*. 2021;14:829–841.
41. Groeneveld CS, Chagas VS, Jones SJM, et al. RTNsurvival: an R/Bioconductor package for regulatory network survival analysis. *Bioinformatics*. 2019;35(21):4488–4489.
42. Kircheis R, Haasbach E, Lueftenegger D, et al. NF-κB pathway as a potential target for treatment of critical stage COVID-19 patients. *Front Immunol*. 2020;11.
43. Mitchell JP, Carmody RJ: Chapter two—NF-κB and the transcriptional control of inflammation. In: Loos F, ed. *International Review of Cell and Molecular Biology* vol. 335. United Kingdom: Academic Press, 2018:41–84.
44. AbdAllah NB, Toraih EA, Al Ageeli E, et al. MYD88, NFKB1, and IL6 transcripts overexpression are associated with poor outcomes and short survival in neonatal sepsis. *Sci Rep*. 2021;11(1):13374.
45. Liu J, Li S, Xiong D, et al. Screening of potential core genes in peripheral blood of adult patients with sepsis based on transcription regulation function. *Shock*. 2023; 59(3):385–392.
46. Li W, Li D, Chen Y, et al. Classic signaling pathways in alveolar injury and repair involved in sepsis-induced ALI/ARDS: new research progress and prospect. *Dis Markers*. 2022;2022:6362344.
47. Shaik F, Cuthbert GA, Homer-Vanniasinkam S, et al. Structural basis for vascular endothelial growth factor receptor activation and implications for disease therapy. *Biomolecules*. 2020;10(12):1673.
48. Ruan G-X, Kazlauskas A. VEGF-A engages at least three tyrosine kinases to activate PI3K/Akt. *Cell Cycle*. 2012;11(11):2047–2048.
49. Karali E, Bellou S, Stellas D, et al. VEGF signaling, mTOR complexes, and the endoplasmic reticulum: towards a role of metabolic sensing in the regulation of angiogenesis. *Mol Cell Oncol*. 2014;1(3):e964024.
50. Zhu H, Gao M, Gao X, et al. Vascular endothelial growth factor-B: impact on physiology and pathology. *Cell Adh Migr*. 2018;12(3):215–227.
51. Zhou Y, Zhu X, Cui H, et al. The role of the VEGF family in coronary heart disease. *Front Cardiovasc Med*. 2021;8.
52. Maruyama K, Kidoya H, Takemura N, et al. Zinc finger protein St18 protects against septic death by inhibiting VEGF-A from macrophages. *Cell Rep*. 2020; 32(2):107906.